Available online at www.sciencedirect.com
ScienceDirect
Journal of Magnetic Resonance 187 (2007) 97–104
JMR Journal of Magnetic Resonance
www.elsevier.com/locate/jmr

Residue-specific NH exchange rates studied by NMR diffusion experiments

Torsten Brand [a], Eurico J. Cabrita [b], Gareth A. Morris [c], Robert Günther [d], Hans-Jörg Hofmann [d], Stefan Berger [a,*]

[a] *Institute of Analytical Chemistry, University of Leipzig, Linnéstraße 3, Leipzig 04103, Germany*
[b] *REQUIMTE/CQFB, Dep. de Química, Faculdada de Ciências e Tecnologia, Univ. Nova de Lisboa, 2829-516 Caparica, Portugal*
[c] *School of Chemistry, University of Manchester, Oxford Road, Manchester M13 9PL, UK*
[d] *Institute of Biochemistry, University of Leipzig, Brüderstraße 34, Leipzig 04103, Germany*

Received 19 September 2006; revised 14 March 2007
Available online 13 April 2007

Abstract

We present a novel approach to the investigation of rapid (>2 s^{-1}) NH exchange rates in proteins, based on residue-specific diffusion measurements. ^{1}H, ^{15}N-DOSY-HSQC spectra are recorded in order to observe resolved amide proton signals for most residues of the protein. Human ubiquitin was used to demonstrate the proposed method. Exchange rates are derived directly from the decay data of the diffusion experiment by applying a model deduced from the assumption of a two-site exchange with water and the ''pure'' diffusion coefficients of water and protein. The ''pure'' diffusion coefficient of the protein is determined in an experiment with selective excitation of the amide protons in order to suppress the influence of magnetization transfer from water to amide protons on the decay data. For rapidly exchanging residues a comparison of our results with the exchange rates obtained in a MEXICO experiment showed good agreement. Molecular dynamics (MD) and quantum mechanical calculations were performed to find molecular parameters correlating with the exchangeability of the NH protons. The RMS fluctuations of the amide protons, obtained from the MD simulations, together with the NH coupling constants provide a bilinear model which shows a good correlation with the experimental NH exchange rates.

Keywords: Exchange; Diffusion; NMR; Ubiquitin; DOSY

1. Introduction

Amide proton exchange rates are of great interest in biochemistry, since they are related to the flexibility and accessibility of different sites in a protein. Mass spectrometry (MS) has been applied to the study of hydrogen–deuterium exchange in proteins [1–4] and in ubiquitin [5,6] in particular. Conformational changes of ubiquitin in methanol solutions [7,8] and partially unfolded states [9] have been investigated using exchange studies by MS. Akashi et al. monitored backbone amide proton exchange in several fragments of ubiquitin [10]. Solvent accessibility of basic side chain protons has also been studied [11]. Early methods for measuring exchange rates by NMR are reviewed in Ref. [12] and have been applied in a variety of studies [13–16]. A water exchange filter (WEX) [17] enables exchange measurements in 1D (and 2D) spectra. Different conformations [18] and the folding process [19,20] of ubiquitin were investigated. Denisov et al. monitored fast exchange of labile side chain protons using ^{2}H spin relaxation [21]. Properties of hydrogen bonds in ubiquitin were also investigated [22]. More recent NMR studies of exchange employ methods for fast data acquisition in order to enable ''real-time'' site-resolved investigations of medium rate exchange in ubiquitin dissolved in D_2O [23–25]. The ability of both MS and NMR to determine hydrogen exchange rates has been used to facilitate the resonance assignment of ^{15}N labelled proteins [26].

* Corresponding author. Fax: +49 341 97 36115.
E-mail address: stberger@rz.uni-leipzig.de (S. Berger).

1090-7807/$ - see front matter © 2007 Elsevier Inc. All rights reserved.
doi:10.1016/j.jmr.2007.03.021

In this paper we present a novel method for the measurement of relatively rapid (>2 s^{-1}) NH exchange rates by NMR, using 3D DOSY-HSQC experiments to measure site-specific diffusional signal attenuation. The use of diffusion experiments to measure NH exchange rates has been reported previously [31]; here, the introduction of a ^{15}N dimension greatly improves resolution.

As is well known, chemically-exchanging systems show anomalous results in PFG diffusion experiments [27–30], spins dividing their time between species diffusing at different rates. Where all exchange is slow compared to the inverse of the magnetization storage delay time Δ_S in a stimulated echo the effects of exchange may be neglected, and each signal shows the attenuation expected for the appropriate diffusion coefficient. Where exchange is fast compared to $1/\Delta_S$, each exchanging signal shows the same attenuation, corresponding to the weighted average of the diffusion coefficients of the exchanging species. In the intermediate case, for two-site exchange the signal attenuation no longer shows a simple exponential dependence on the square of field gradient pulse area, but rather the sum of two exponentials, neither of which is a simple function of the experimental parameters; the deviation from monoexponential behavior is at its greatest for rate constants of the order of $1/\Delta_S$. Johnson's general analysis of the effects of exchange during Δ_S [30] is extended in Appendix A to include the effects of relaxation, and a simplified version appropriate to the experiments described here, where one exchange partner (water) is in large excess, is derived.

For a bipolar stimulated echo sequence of the type used here (Fig. 1), if the times τ and Δ_S are sufficiently short that the effects of relaxation can be neglected, the attenuation of the NH signal $S_N(K)$ as a function of the degree of diffusion encoding $K = \gamma g \delta$ is given (see Eq. (A17a) in Appendix A) by

$$S_N(K) = S_N(0)e^{-D_N K^2\left(\tau-\frac{\delta}{3}-\frac{\tau'}{2}\right)} \times \left[e^{-\left(k_{NW}+D_N K^2\right)\Delta_S} + \frac{k_{NW}}{k_{NW}+D_N K^2 - D_W K^2} \times \left(e^{-D_W K^2 \Delta_S} - e^{-\left(k_{NW}+D_N K^2\right)\Delta_S}\right)\right] \quad (1)$$

where γ is the proton magnetogyric ratio, g the applied gradient strength, δ the net effective duration of the (two bipolar) gradient pulses, k_{NW} the exchange rate constant from NH to water, D_N and D_W the protein and water diffusion coefficients, respectively, τ the diffusion-en/decoding delay and τ' the time between the midpoints of the two bipolar gradient pulses. For half-sine shaped pulses the correction term for diffusion during the gradient pulses changes from $\delta/3$ to $\delta/4$.

2. Experimental

A 1.8 mM solution of uniformly ^{13}C, ^{15}N-labelled human ubiquitin (90% H_2O/10% D_2O in pH 5.8 phosphate buffer) was used in this study, since for this relatively small protein (76 residues, MW = 9.0 kDa) the resonance assignment [32–34] and NMR structure [35] are available, facilitating the assignment of signals and the subsequent interpretation of results. All experiments were performed at 297K on a Bruker Avance 700 equipped with a cryo probehead. TopSpin 2.0 was used for recording and data processing. Gradient calibration was performed by recording an image of the water distribution in an NMR tube containing a Teflon disk of known thickness [36]. Comparison between experiments using the double stimulated echo [37] (DSTE) technique and the "normal" stimulated echo (STE) sequence under otherwise identical conditions showed that no convection compensation was needed.

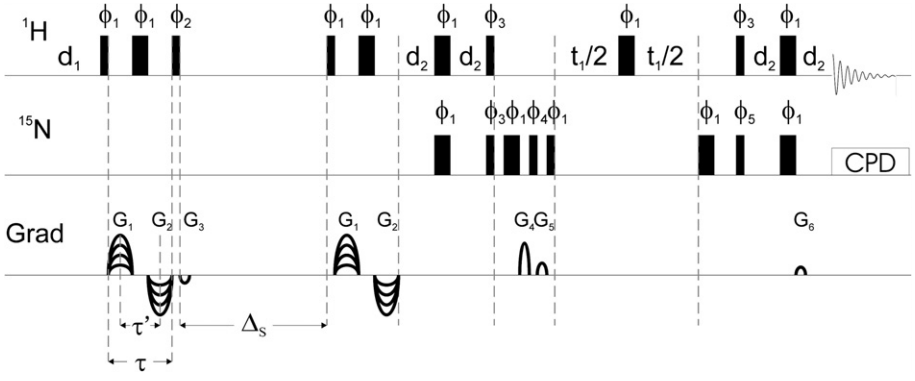

Fig. 1. Pulse scheme for the 3D ^1H, ^{15}N-DOSY-HSQC experiment (without applying DSTE). Narrow and wide filled rectangles denote 90° and 180° pulses, respectively. The ^{15}N offset was centered in the amide region (118 ppm), ^1H offset was set to the center of NH resonances (7.75 ppm). A diffusion time (Δ) of 80 ms was used for the determination of the exchange rates. The figure shows the effective diffusion time and not the technical delay. d_1 represents the relaxation delay (12 s). INEPT transfers were carried out using a delay of $d_2 = 1/(4 \times J_{NH}) = 2.63$ ms. The incremented delay for the evolution of ^{15}N chemical shifts is represented by t_1. 800 and 256 data points were acquired in the ^1H and ^{15}N dimensions, respectively. During acquisition ^{15}N GARP decoupling was applied. Phase cycles were $\phi_1 = x$; $\phi_2 = 4(x)$, $4(-x)$; $\phi_3 = y$; $\phi_4 = -y$; $\phi_5 = x$, $-x$; receiver = x, $-x$, x, $2(-x)$, x, $-x$, x. Gradients were half-sine shaped (100 data points) and have the following durations and peak amplitudes: G_1: 2.5 ms, 6.6 to 46.2 G × cm^{-1}, varied in nine steps; G_2: 2.5 ms, −6.6 to −46.2 G cm^{-1}, varied in nine steps; G_3: 1 ms, −9.4 G cm^{-1}; G_4: 1 ms, 44.0 G cm^{-1}; G_5: 1 ms, 16.5 G cm^{-1}; G_6: 1 ms, 4.5 G cm^{-1}. For the determination of D_N the first ^1H pulse was replaced by a 3 ms Gaussian cascade [39] pulse (G^4; 256 data points) centered in the middle of the amide region (7.75 ppm) to excite selectively the NH protons. The time intervals relevant for data analysis are indicated.

The water diffusion coefficient, D_W, in the protein sample, measured at the experimental temperature using a standard BPPLED [38] diffusion experiment with $\Delta = 30$ ms and $\delta = 3$ ms, was 1.96×10^{-9} m^2 s^{-1}.

The 3D ^{1}H, ^{15}N-DOSY-HSQC sequence used (for graphical description and further experimental details, see Fig. 1) concatenates a bipolar pulse pair stimulated echo sequence [38] (BPPSTE) with an ^{1}H, ^{15}N-HSQC sequence, and yields a 3D data matrix. A diffusion time Δ of 80 ms was used, with nine different gradient strengths. For the determination of the protein diffusion coefficient, D_N, the sequence was changed to excite only the amide protons and not the water, using a 3 ms Gaussian cascade [39] pulse (G^4; 256 datapoints) centered at 7.75 ppm in the middle of the amide region. Because only the protein magnetization is position-encoded, despite the water being in large excess, the water contribution to the diffusional attenuation of the NH signals is suppressed. In this experiment the diffusion coefficients of all assignable amide protons of ubiquitin were found to be equal within experimental error, with an average of 1.35×10^{-10} m^2 s^{-1}. For comparison purposes, a ^{1}H, ^{13}C-DOSY-HSQC spectrum (using WURST [40] decoupling to minimize sample heating) was recorded as a control experiment, and gave the same result. A long relaxation delay (12 s) was used to ensure complete water relaxation between transients, but, as expected from the form of Eq. (1) in which the value of the (large) NH:water equilibrium constant is immaterial, experiments with much shorter recycle delays give essentially the same results.

The ^1J(NH) coupling constants were determined in a ^{1}H, ^{15}N-HSQC experiment without decoupling during acquisition and with a digital resolution of 0.1 Hz in the proton dimension.

For all theoretical studies, the PDB dataset 1D3Z for ubiquitin was used as starting point [35]. The quantum chemical studies were performed employing the semiempirical MNDO method. Molecular dynamics (MD) simulations on ubiquitin were done over 10 ns on the basis of the empirical force field CHARMm23.1, considering the solvent water implicitly by its dielectric constant. From the results, we extracted a variety of parameters thought to be possible indicators for the exchangeability of the amide protons (vide infra).

3. Results and discussion

In contrast to the amide-selective experiment, in which the effects of exchange with water were suppressed, the parent 3D DOSY-HSQC sequence gave NH signal attenuation that varied markedly from site to site, confirming the presence of significant exchange between water and protein NH magnetization. Apparent diffusion coefficients obtained by fitting the selective and non-selective experiment decays to the Stejskal–Tanner equation are reported in Fig. A1; in the latter case, significant systematic deviations from exponential decay were seen, as expected from Eq. (1).

The NH signal decays from the non-selective experiment were analysed directly to extract apparent exchange rate constants k_{NW}. Published chemical shifts [34] were used for the resonance assignment. The TopSpin 2D integration routine was applied to 2D slices of the pseudo 3D spectrum using identical, non-overlapping regions for all gradient strengths. ORIGIN™ 6.1 was used for non-linear least squares fitting of the signal intensities obtained for different gradient strengths (K values) according to Eq. (1), with initial signal integral $S_N(0)$ and k_{NW} as parameters.

The amide magnetization exchange rates obtained for ubiquitin are shown in Fig. 2. Whereas the vast majority of residues show slow exchange (rate constants below 2 s^{-1}) a number of amide protons exchange significantly faster (e.g., Gly 75, Thr 9, Arg 74, Ala 46). This is not unexpected, since all of these are located outside of α-helices and β-sheets and are assigned to bends, turns [35] or the C terminus. They are therefore less stabilized by hydrogen bonds, more easily accessible to water, and prone to more rapid exchange.

Very slow (<10 h^{-1}) NH exchange in proteins is relatively easy to monitor using dissolution experiments [41], and as has already been noted, rapid acquisition methods can extend the scope of this method to rate constants greater than 1 min^{-1} [23–25]. The method described here, in contrast, is intended for probing processes at the upper end of the range of amide exchange rates, with rate constants of several s^{-1} and above. The lower limit of such methods is set by competition between the chemical exchange of magnetization (between NH and water) and the exchange of magnetization by cross-relaxation. There is a direct analogy between the study of two-site exchange processes here and the use of the NOE in the structure elucidation of biomolecules: in both cases there is competition

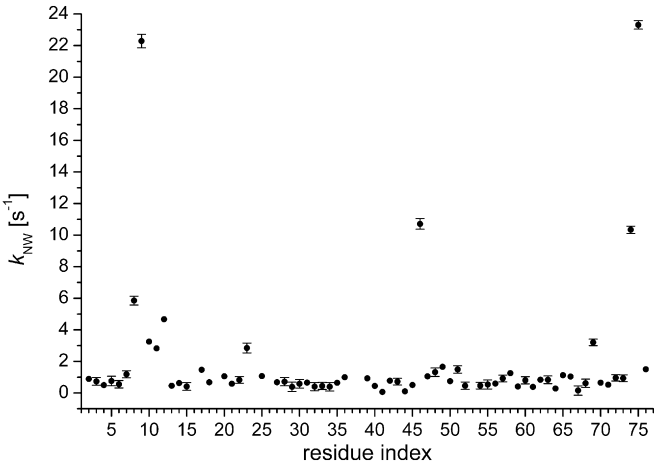

Fig. 2. Magnetization exchange rates for most amide protons of ubiquitin obtained by the proposed diffusion-based method. The error bars represent the standard deviations of the exchange rates obtained in the fitting procedure. Data points with no displayed error bars show uncertainties which are smaller than or in the order of the size of the filled circles (ca. 0.2 s^{-1}). For precise numbers, error margins for all residues and for experimental details, see Table A1.

between two-site processes and spin diffusion, and in both cases the trade-off between the two is partly under the control of the experimenter, through the choice of the delay Δ_S and the NOE mixing period, respectively. Under the experimental conditions used here, the effect of spin diffusion transmitting the effects of exchange at rapidly-exchanging sites throughout the protein is to give an apparent "background" exchange rate of about $0.3\ s^{-1}$. The results reported in Table A1 for apparent k_{NW} are the raw results of fitting the experimental data to Eq. (1); the true exchange rates are better approximated by subtracting the background apparent exchange rate. For the residues that these experiments are intended to probe (those with $k_{NW} > 2\ s^{-1}$) this correction is typically of the order of or smaller than the random error estimated from the fitting.

To assess the validity of our method comparative experiments were performed on the same sample using the MEXICO sequence [42] with nine different mixing times ranging from 25 to 300 ms. Due to radiation damping effects observed with the cryoprobe, the original phase cycling had to be altered and could therefore no longer provide compensation for T_1 relaxation effects. For rapidly exchanging amide protons the rates determined by MEXICO were comparable to ours; for slower exchange the MEXICO data did not yield unambiguous exchange rates, suggesting that at slower exchange rates the diffusion method may have an advantage over MEXICO. In the Appendices the correlation between the exchange rates obtained by the two methods can be seen graphically (Fig. A2) and numerically (Table A2).

Computational studies can also be used to investigate dynamic processes in proteins [43]. To gain insight into the molecular basis of the exchange behavior, we performed molecular dynamics and quantum chemical studies and tried to find molecular parameters from theory and NMR measurements correlating with the exchangeability of the NH protons. For example, the fluctuations of the NH atoms around the average molecular structure obtained from the MD simulations reflect the accessibility of the protons for exchange. Such information can also be obtained from the accessible surface areas of the NH protons calculated on the basis of the experimental molecular structure. The extent of the involvement of the exchangeable NH protons in hydrogen bonds, which can also be obtained from the MD trajectories, represents another parameter reflecting exchangeability. Finally, the quantum-chemically calculated bond orders of the N–H bonds could be regarded as a measure of the N–H bond strength, and the charges at the peptidic nitrogen atoms as a measure of basicity.

Due to the large relative uncertainties in k_{NW} for slowly exchanging residues, only the six most rapidly exchanging amide protons were taken into account when looking for correlations. No single parameter of those mentioned above gave a direct quantitative correlation with the experimental k_{NW} values, but a bilinear model based on the fluctuations of the NH protons and on the NH coupling constants provides a fair correlation between predicted and measured exchange rates, with a regression coefficient of 0.965, as shown in Fig. 3.

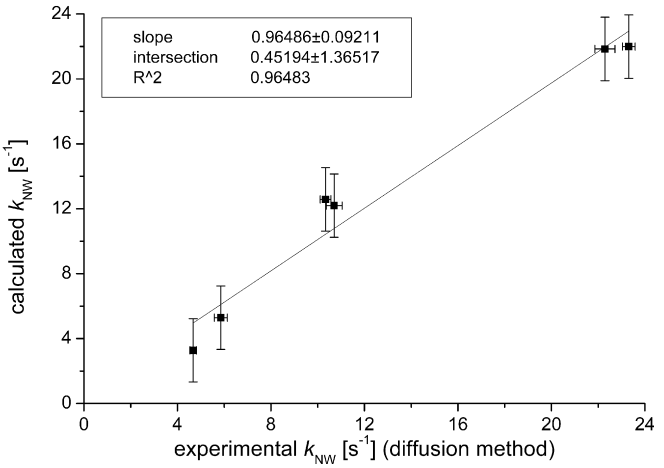

Fig. 3. Correlation between the experimental exchange rates for the fastest exchanging amide protons and those calculated with a bilinear model, which is characterized by the equation: $k_{NW}^{pred}/s^{-1} = a \cdot f_{NH} + b \cdot J_{NH} + c$, where f_{NH} represents the RMS fluctuations of the NH protons around the avarage structure during the MD simulation (in Å) and J_{NH} represents the coupling constant between the amide proton and nitrogen (in Hz). The coefficients are $a = 90.1 \pm 10.2$; $b = -5.25 \pm 0.73$, and $c = 426.8 \pm 62.8$. The regression coefficient is 0.965. The horizontal error bars represent the statistical error obtained during fitting the experimental data to Eq. (1), whereas the vertical error bars represent the standard error of estimate of our bilinear model ($1.81\ s^{-1}$).

4. Conclusions

In conclusion, we have shown that ^1H, ^{15}N-DOSY-HSQC experiments are a powerful tool for the quantification of fast ($>2\ s^{-1}$) amide proton exchange rates, which should be generally applicable to proteins with well-resolved ^1H, ^{15}N-HSQC signals. The method is not restricted to chemical exchange [44]; the approach used here could for example provide a quantitative basis for epitope mapping [45]. Most recently, a paper was published in which by a very different method the amino acids Thr 9, Ala 46 and Gly 75 also show strongly enhanced NH exchange [46].

Acknowledgments

We gratefully acknowledge financial support by SFB 610 (Deutsche Forschungsgemeinschaft; T.B., R.G., H.J.H., S.B.) and by EPSRC (GR/S90751, GAM).

Appendix A

For two-site exchange, the signal attenuation in a PFG-STE experiment has been analysed in detail by Johnson [30]. Johnson's analysis describes the signal behavior as a function of the longitudinal magnetization storage period

Δ_S of the stimulated echo experiment. In an exchanging system the signal attenuation no longer shows a simple exponential dependence on the square K^2 of the effective field gradient pulse area, but rather a mixture of two exponentials, neither of which is a simple function of the experimental parameters, in which the relative contributions of the two exponentials vary with K^2. The deviation from monoexponential behavior is at its greatest for rate constants of the order of $1/\Delta_S$.

For two longitudinal magnetizations A and B with equilibrium values M_0^A and M_0^B and initial values at the start of the Δ_S delay $M_z^A(0)$ and $M_z^B(0)$, exchanging with rate constants k_A and k_B such that $k_A M_0^A = k_B M_0^B$ and diffusing with diffusion coefficients D_A and D_B, respectively, then neglecting relaxation and exchange and diffusion during the diffusion-encoding and decoding periods, the resultant contributions to the net magnetizations at the end of a PFGSTE sequence are given [30] by

$$\begin{aligned} M_z^A(K,\Delta_S) = &\left[\frac{M_z^A(0)}{2} - \frac{\{\lambda M_z^A(0) - k_B M_z^B(0)\}}{2R}\right] \\ &\times \exp[(-\sigma + R)\Delta_S] \\ &+ \left[\frac{M_z^A(0)}{2} + \frac{\{\lambda M_z^A(0) - k_B M_z^B(0)\}}{2R}\right] \\ &\times \exp[(-\sigma - R)\Delta_S] \end{aligned} \tag{A1}$$

$$\begin{aligned} M_z^B(K,\Delta_S) = &\left[\frac{M_z^B(0)}{2} + \frac{\{\lambda M_z^B(0) + k_A M_z^A(0)\}}{2R}\right] \\ &\times \exp[(-\sigma + R)\Delta_S] \\ &+ \left[\frac{M_z^B(0)}{2} - \frac{\{\lambda M_z^B(0) + k_A M_z^A(0)\}}{2R}\right] \\ &\times \exp[(-\sigma - R)\Delta_S] \end{aligned} \tag{A2}$$

where

$$\sigma = \tfrac{1}{2}\left(k_A + k_B + D_A K^2 + D_B K^2\right) \tag{A3}$$

$$\lambda = \tfrac{1}{2}\left(k_A - k_B + D_A K^2 - D_B K^2\right) \tag{A4}$$

$$R = \sqrt{\lambda^2 + k_A k_B} \tag{A5}$$

and $K = \gamma g \delta$ is the product of the magnetogyric ratio, the duration and the amplitude of the (rectangular) diffusion-encoding gradient pulses. The quantities δ and Δ in Johnson's analysis have been replaced here by λ and R to avoid confusion with the gradient pulse width and magnetization storage delay, respectively. Note that the magnetizations that eventually refocus in the stimulated echo are reduced by a further factor of 2.

The effects of spin–lattice relaxation during the diffusion delay, neglected in Johnson's analysis, are straightforward to include, the expressions for σ and λ becoming

$$\sigma = \tfrac{1}{2}\left(k_A + k_B + R_1^A + R_1^B + D_A K^2 + D_B K^2\right) \tag{A3a}$$

$$\lambda = \tfrac{1}{2}\left(k_A - k_B + R_1^A - R_1{}^B + D_A K^2 - D_B K^2\right) \tag{A4a}$$

where R_1^A and R_1^B are the inverses of the spin–lattice relaxation times T_1 for A and B, respectively.

The effects of exchange and relaxation during the diffusion-encoding and decoding delays are also straightforward to include if exchange is slow on the chemical shift timescale, i.e., if the rate constants are small compared to the chemical shift difference between the two-sites. Under such conditions the effect of chemical exchange on transverse magnetization is simply a net loss of coherence, and the two exchanging magnetizations evolve independently; only as coalescence approaches is there net transfer of magnetization from one-site to another. If the diffusion-encoding and decoding periods each consist of a single gradient pulse of width δ at the midpoint of a delay τ, the contributions M_{xy}^A and M_{xy}^B made by the transverse magnetizations to the final echo signal decay according to

$$M_{xy}^A = M_{xy}^A(0) E_{2A} \tag{A6}$$

$$M_{xy}^B = M_{xy}^B(0) E_{2B} \tag{A7}$$

where

$$E_{2A} = e^{-R_2^A \tau - k_A \tau - \frac{1}{2} D_A K^2 \left(\tau - \frac{\delta}{3}\right)} \tag{A8}$$

$$E_{2B} = e^{-R_2^B \tau - k_B \tau - \frac{1}{2} D_B K^2 \left(\tau - \frac{\delta}{3}\right)} \tag{A9}$$

and where $M_{xy}^A(0)$ is the transverse magnetization at the beginning of a given period τ and R_2^A and R_2^B are the inverses of the spin–spin relaxation times T_2 for A and B, respectively. For sequences with bipolar diffusion-encoding and decoding, using two gradient pulses of opposite polarity with widths $\delta/2$ and midpoints τ' apart at the middle of a delay τ, the expressions become

$$E_{2A} = e^{-R_2^A \tau - k_A \tau - \frac{1}{2} D_A K^2 \left(\tau - \frac{\delta}{3} - \frac{\tau'}{2}\right)} \tag{A8a}$$

$$E_{2B} = e^{-R_2^B \tau - k_B \tau - \frac{1}{2} D_B K^2 \left(\tau - \frac{\delta}{3} - \frac{\tau'}{2}\right)} \tag{A9a}$$

For perfect 90° pulses, then neglecting resonance offset and spatial encoding (which are refocused in the stimulated echo, the latter effect sacrificing half of the net signal) the magnitudes of the initial spatially-encoded longitudinal magnetizations at the start of Δ_S are equal to those of the transverse magnetizations in Eqs. (A6) and (A7), and the magnitudes of the final magnetizations M_{xy}^A that refocus in the stimulated echo may be obtained by substituting (A6) and (A7) into (A1) and (A2), dividing by 2 as noted earlier, and weighting for the effects of diffusion, exchange and relaxation during the final diffusion decoding delay τ:

$$\begin{aligned} M_{xy}^A = &\left[\frac{M_0^A E_{2A}}{4} - \frac{\{\lambda M_0^A E_{2A} - k_B M_0^B E_{2B}\}}{4R}\right] \\ &\times \exp[(-\sigma + R)\Delta_S] E_{2A} \\ &+ \left[\frac{M_0^A E_{2A}}{4} + \frac{\{\lambda M_0^A E_{2A} - k_B M_0^B E_{2B}\}}{4R}\right] \\ &\times \exp[(-\sigma - R)\Delta_S] E_{2A} \end{aligned} \tag{A10}$$

$$M_{xy}^{B} = \left[\frac{M_0^B E_{2B}}{4} + \frac{\{\lambda M_0^B E_{2B} + k_A M_0{}^A E_{2A}\}}{4R}\right] \times \exp\left[(-\sigma + R)\Delta_S\right]E_{2B} + \left[\frac{M_0^B E_{2B}}{4} - \frac{\{\lambda M_0^B E_{2B} + k_A M_0^A E_{2A}\}}{4R}\right] \times \exp\left[(-\sigma - R)\Delta_S\right]E_{2B} \quad \text{(A11)}$$

For the asymmetric case where the two-site equilibrium lies far to one side, as in the exchange of magnetization between protein NH groups (A) and water (B), considerable simplifications are possible. If the B pool is much larger than the A, and if differential attenuation between A and B during the diffusion-encoding delay is small (both conditions being met in the experiments described here), then $k_A \gg k_B$, $E_{2A} \approx E_{2B}$ and $k_A M_z^A(0) \approx k_B M_z^B(0)$, causing Eqs. (A10) and (A11) above to reduce to

$$M_{xy}^{A} = \frac{1}{2}M_A^0\left[E_{1A} + \frac{k_A}{2\lambda}(E_{1B} - E_{1A})\right]E_{2A}^2 \quad \text{(A12)}$$

$$M_{xy}^{B} = \tfrac{1}{2}M_B^0 E_{1B}E_{2B}^2 \quad \text{(A13)}$$

where

$$\lambda = \tfrac{1}{2}\left(k_A + R_1^A - R_1^B + D_A K^2 - D_B K^2\right) \quad \text{(A14)}$$

$$E_{1A} = \exp\left[-\left(k_A + R_1^A + D_A K^2\right)\Delta_S\right] \quad \text{(A15)}$$

$$E_{1B} = \exp\left[-\left(R_1^B + D_B K^2\right)\Delta_S\right] \quad \text{(A16)}$$

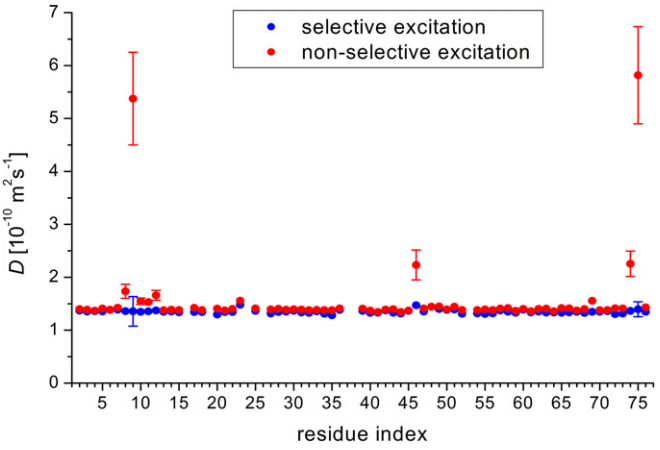

Fig. A1. Comparison of the (apparent) diffusion coefficients D obtained with selective excitation of the amide region by a Gaussian cascade (G^4) pulse centered at 7.75 ppm with 3 ms duration (blue circles) and with excitation of all protons (red circles). D was calculated by non-linear least squares fitting of the respective decay data according to $I = I_0 \times \exp(-DK^2(\Delta - \delta/4 - \tau'/2))$, where I is the gradient strength dependent signal intensity, I_0 is the (hypothetical) signal intensity with no applied gradient, and the other symbols are explained in the main text. The error bars represent the standard deviation of the diffusion coefficients provided by the fitting routine. For all data points with no displayed error bar the uncertainty is lower than the extension of the points (ca. 0.06×10^{-10} m^{2}s^{-1}). For all residues, uniform excitation yields slightly higher apparent diffusion coefficients. This discrepancy is probably due to spin diffusion within the protein. Expectedly, fast exchanging protons show much larger differences in D between both experiments.

Table A1
Magnetization exchange rates k_{NW} of the NH protons in human ubiquitin obtained by fitting to Eq. (1)

Residue	k_{NW} [s^{-1}]	$\sigma(k_{NW})$ [s^{-1}]
Gln 2	0.89	0.17
Ile 3	0.73	0.24
Phe 4	0.50	0.13
Val 5	0.76	0.30
Lys 6	0.55	0.23
Thr 7	1.19	0.23
Leu 8	5.86	0.28
Thr 9	22.29	0.43
Gly 10	3.25	0.13
Lys 11	2.83	0.16
Thr 12	4.67	0.14
Ile 13	0.46	0.19
Thr 14	0.63	0.19
Leu 15	0.41	0.24
Val 17	1.47	0.14
Glu 18	0.68	0.13
Ser 20	1.06	0.12
Asp 21	0.59	0.17
Thr 22	0.83	0.21
Ile 23	2.85	0.31
Asn 25	1.07	0.14
Lys 27	0.68	0.19
Ala 28	0.71	0.26
Lys 29	0.39	0.30
Ile 30	0.58	0.27
Gln 31	0.66	0.19
Asp 32	0.40	0.26
Lys 33	0.45	0.22
Glu 34	0.40	0.27
Gly 35	0.65	0.19
Ile 36	1.00	0.18
Asp 39	0.93	0.20
Gln 40	0.45	0.12
Gln 41	0.07	0.13
Arg 42	0.78	0.17
Leu 43	0.72	0.21
Ile 44	0.11	0.17
Phe 45	0.51	0.13
Ala 46	10.71	0.34
Gly 47	1.06	0.20
Lys 48	1.32	0.27
Gln 49	1.66	0.18
Leu 50	0.75	0.16
Glu 51	1.49	0.23
Asp 52	0.46	0.23
Arg 54	0.47	0.21
Thr 55	0.54	0.29
Leu 56	0.60	0.17
Ser 57	0.92	0.21
Asp 58	1.26	0.15
Tyr 59	0.41	0.15
Asn 60	0.80	0.23
Ile 61	0.38	0.19
Gln 62	0.84	0.18
Lys 63	0.83	0.24
Glu 64	0.29	0.12
Ser 65	1.13	0.17
Thr 66	1.04	0.20
Leu 67	0.16	0.29
His 68	0.62	0.27
Leu 69	3.21	0.20
Val 70	0.65	0.15
Leu 71	0.52	0.20

Table A1 (*continued*)

Residue	k_{NW} [s^{-1}]	$\sigma(k_{NW})$ [s^{-1}]
Arg 72	0.96	0.20
Leu 73	0.93	0.22
Arg 74	10.34	0.23
Gly 75	23.31	0.27
Gly 76	1.51	0.09

The indicated standard deviation $\sigma(k_{NW})$ results from the fitting procedure which was performed using Origin™ 6.1. Residues missing in this table are proline (Pro 19, Pro 37, Pro 38) or could not be evaluated due to signal overlap.

Note that care is needed in numerical evaluation of the second term in the expression for $M_z^A(K, \Delta_S)$ in Eq. (A1) near the point where the quantities λ and $(E_{1B} - E_{1A})$ both change sign.

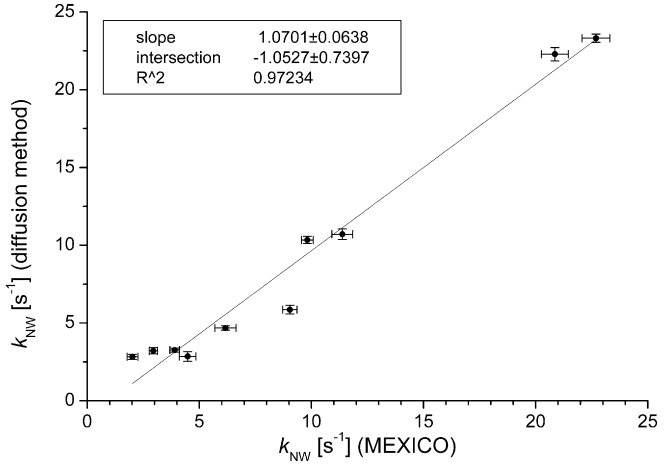

Fig. A2. Comparison of exchange rates obtained using the MEXICO [42] pulse sequence to those derived from the proposed diffusion-based method. Ten residues which yielded unambiguous MEXICO results (i.e., those with the highest exchange rates) were taken into account. For precise numbers as well as uncertainties obtained in the fitting procedure see Table A2.

Table A2
Exchange rates k_{NW} of the fastest exchanging amide protons in human ubiquitin obtained by the MEXICO experiment [42] in comparison to those obtained by the proposed diffusion-based method with subsequent fitting to Eq. (1)

	MEXICO experiment		Diffusion based method	
	k_{NW} [s^{-1}]	$\sigma(k_{NW})$ [s^{-1}]	k_{NW} [s^{-1}]	$\sigma(k_{NW})$ [s^{-1}]
Gly 75	22.69	0.62	23.31	0.27
Thr 9	20.86	0.60	22.29	0.43
Ala 46	11.38	0.46	10.71	0.34
Arg 74	9.82	0.27	10.34	0.23
Leu 8	9.04	0.32	5.86	0.28
Thr 12	6.17	0.48	4.67	0.14
Gly 10	3.90	0.21	3.25	0.13
Leu 69	2.95	0.18	3.21	0.20
Ile 23	4.48	0.37	2.85	0.31
Lys 11	2.02	0.24	2.83	0.16

The indicated standard deviations for both methods ($\sigma(k_{NW})$) result from the fitting procedures which were performed using Origin™ 6.1.

Thus, if the effects of relaxation during the sequence are small, the experimental signal $S_A(K)$ for site A in a simple PFGSTE experiment should attenuate with K according to

$$S_A(K) = S_A(0)\left[e^{-\left(k_A + D_A K^2\right)\Delta_S} + \frac{k_A}{k_A + D_A K^2 - D_B K^2} \times \left(e^{-D_B K^2 \Delta_S} - e^{-\left(k_A + D_A K^2\right)\Delta_S}\right)\right] e^{-D_A K^2\left(\tau - \frac{\delta}{3}\right)} \quad \text{(A17)}$$

and in a bipolar experiment according to

$$S_A(K) = S_A(0)\left[e^{-(k_A + D_A K^2)\Delta_S} + \frac{k_A}{k_A + D_A K^2 - D_B K^2} \times \left(e^{-D_B K^2 \Delta_S} - e^{-\left(k_A + D_A K^2\right)\Delta_S}\right)\right] e^{-D_A K^2\left(\tau - \frac{\delta}{3} - \frac{\gamma}{2}\right)} \quad \text{(A17a)}$$

in which the only unknown parameters are k_A and $S_A(0)$.

References

[1] V. Katta, B.T. Chait, Conformational changes in proteins probed by hydrogen-exchange electrospray-ionization mass spectrometry, Rapid Commun. Mass Spectrom. 5 (1991) 214–217.
[2] J.R. Engen, E.M. Bradbury, X. Chen, Using stable-isotope-labeled proteins for hydrogen-exchange studies in complex mixtures, Anal. Chem. 74 (2002) 1680–1686.
[3] J.R. Engen, Analysis of protein complexes with hydrogen exchange and mass spectrometry, Analyst 128 (2003) 623–628.
[4] S.J. Eyles, I.A. Kaltashov, Methods to study protein dynamics and folding by mass spectrometry, Methods 34 (2004) 88–99.
[5] M.A. Freitas, C.L. Hendrickson, M.R. Emmett, A.G. Marshall, Gas-phase bovine ubiquitin cation conformations resolved by gas-phase hydrogen/deuterium exchange rate and extent, Int. J. Mass Spectrom. 185/186/187 (1999) 565–575.
[6] S.E. Evans, N. Lueck, E.M. Marzluff, Gas phase hydrogen/deuterium exchange of proteins in an ion trap mass spectrometer, Int. J. Mass Spectrom. 222 (2003) 175–187.
[7] V. Katta, B.T. Chait, Hydrogen/deuterium exchange electrospray ionization mass spectrometry: a method for probing protein conformational changes in solution, J. Am. Chem. Soc. 115 (1993) 6317–6321.
[8] K.R. Babu, A. Moradian, D.J. Douglas, The methanol-induced conformational transitions of β-lactoglobulin, cytochrome *c*, and ubiquitin at low pH: a study by electrospray ionization mass spectrometry, J. Am. Soc. Mass Spectrom. 12 (2001) 317–328.
[9] J.K. Hoerner, H. Xiao, I.A. Kaltashov, Structural and dynamic characteristics of a partially folded state of ubiquitin revealed by hydrogen exchange mass spectrometry, Biochemistry 44 (2005) 11286–11294.
[10] S. Akashi, Y. Naito, K. Takio, Observation of hydrogen–deuterium exchange of ubiquitin by direct analysis of electrospray capillary-skimmer dissociation with fourier transform ion cyclotron resonance mass spectrometry, Anal. Chem. 71 (1999) 4974–4980.
[11] P. Novak, G.H. Kruppa, M.M. Young, J. Schoeniger, A Top–down method for the determination of residue-specific solvent accessibility in proteins, J. Mass Spectrom. 39 (2004) 322–328.
[12] S.W. Englander, L. Mayne, Protein folding studied using hydrogen-exchange labeling and two-dimensional NMR, Annu. Rev. Biophys. Biomol. Struct. 21 (1992) 243–265.
[13] G. Wagner, K. Wüthrich, Amide proton exchange and surface conformation of the basic pancreatic trypsin inhibitor in solution, J. Mol. Biol. 160 (1982) 343–361.
[14] M. Delepierre, C.M. Dobson, M. Karplus, F.M. Poulsen, D.J. States, R.E. Wedin, Electrostatic effects and hydrogen exchange behaviour in proteins: the ph dependence of exchange rates in lysozyme, J. Mol. Biol. 197 (1987) 111–130.

[15] H. Roder, G.A. Elöve, S.W. Englander, Structural characterization of folding intermediates in cytochrome *c* by H-exchange labelling and proton NMR, Nature 335 (1988) 700–704.
[16] S. Grzesiek, A. Bax, Measurement of amide proton exchange rates and NOEs with water in $^{13}C/^{15}N$-enriched calcineurin B, J. Biomol. NMR 3 (1993) 627–638.
[17] S. Mori, M. O'Neil Johnson, J.M. Berg, P.C.M. van Zijl, Water exchange filter (WEX Filter) for nuclear magnetic resonance studies of macromolecules, J. Am. Chem. Soc. 116 (1994) 11982–11984.
[18] Y. Pan, M.S. Briggs, Hydrogen exchange in native and alcohol forms of ubiquitin, Biochemistry 31 (1992) 11405–11412.
[19] M.S. Briggs, H. Roder, Early hydrogen-bonding events in the folding reaction of ubiquitin, Proc. Natl. Acad. Sci. USA 89 (1992) 2017–2021.
[20] D.P. Nash, J. Jonas, Structure of the pressure-assisted cold denatured state of ubiquitin, Biochem. Biophys. Res. Commun. 238 (1997) 289–291.
[21] V.P. Denisov, B. Halle, Hydrogen exchange and protein hydration: the deuteron spin relaxation dispersions of bovine pancreatic trypsin inhibitor and ubiquitin, J. Mol. Biol. 245 (1995) 698–709.
[22] F. Cordier, S. Grzesiek, Temperature-dependence of protein hydrogen bond properties as studied by high-resolution NMR, J. Mol. Biol. 715 (2002) 739–752.
[23] C. Bougault, L. Feng, J. Glushka, E. Kupče, J.H. Prestegard, Quantitation of rapid proton–deuteron amide exchange using hadamard spectroscopy, J. Biomol. NMR 28 (2004) 385–390.
[24] P. Schanda, B. Bru tscher, Very fast two-dimensional nmr spectroscopy for real-time investigation of dynamic events in proteins on the time scale of seconds, J. Am. Chem. Soc. 127 (2005) 8014–8015.
[25] M. Gal, M. Mishkovsky, L. Frydman, Real-time monitoring of chemical transformations by Ultrafast 2D NMR spectroscopy, J. Am. Chem. Soc. 128 (2006) 951–956.
[26] L. Feng, R. Orlando, J.H. Prestegard, Mass spectrometry assisted assignment of NMR resonances in ^{15}N labeled proteins, J. Am. Chem. Soc. 126 (2004) 14377–14379.
[27] K.F. Morris, C.S. Johnson, Diffusion-ordered two-dimensional nuclear magnetic resonance spectroscopy, J. Am. Chem. Soc. 114 (1992) 3139–3141.
[28] J.E. Tanner, Use of the stimulated echo in NMR diffusion studies, J. Chem. Phys. 25 (1970) 2523–2526.
[29] E.J. Cabrita, S. Berger, P. Bräuer, J. Kärger, High-resolution DOSY NMR with spins in different chemical surroundings: influence of particle exchange, J. Magn. Reson. 157 (2002) 124.
[30] C.S. Johnson Jr., Effects of chemical exchange in diffusion-ordered 2D NMR spectra, J. Magn. Reson. A102 (1993) 214–218.
[31] A. Böckmann, E. Guittet, Determination of fast proton exchange rates of biomolecules by NMR using water selective diffusion experiments, FEBS Lett. 418 (1997) 127–130.
[32] P.F. Flynn, M.J. Milton, C.R. Babu, A.J. Wand, A simple and effective NMR cell for studies of encapsulated proteins dissolved in low viscosity solvents, J. Biomol. NMR 23 (2002) 311–316.
[33] A.C. Wang, S. Grzesiek, R. Tschudin, P.J. Lodi, A. Bax, Sequential backbone assignment of isotopically enriched proteins in D_2O by deuterium-decoupled HA(CA)N and HA(CACO)N, J. Biomol. NMR 5 (1995) 376–382.
[34] A.J. Wand, J.L. Urbauer, R.P. McEvoy, R.J. Bieber, Internal dynamics of human ubiquitin revealed by ^{13}C-relaxation studies of randomly fractionally labeled protein, Biochemistry 35 (1996) 6116–6125.
[35] G. Cornilescu, J.L. Marquardt, M. Ottiger, A. Bax, Validation of protein structure from anisotropic carbonyl chemical shifts in a dilute liquid crystalline phase, J. Am. Chem. Soc. 120 (1998) 6836–6837.
[36] S. Berger, S. Braun, 200 and More NMR Experiments, A Practical Course, Wiley-VCH, Weinheim, 2005.
[37] A. Jerschow, N. Müller, Suppression of convection artifacts in stimulated-echo diffusion experiments. Double-stimulated-echo experiments, J. Magn. Reson. 125 (1997) 372–375.
[38] D. Wu, A. Chen, C.S. Johnson Jr., An improved diffusion-ordered spectroscopy experiment incorporating bipolar-gradient pulses, J. Magn. Reson. A 115 (1995) 260–264.
[39] L. Emsley, G. Bodenhausen, Gaussian pulse cascades: new analytic functions for rectangular selective inversion and in-phase excitation in NMR, Chem. Phys. Lett. 165 (1990) 469–476.
[40] E. Kupče, R. Freeman, Adiabatic pulses for wideband inversion and broadband decoupling, J. Magn. Reson. A115 (1995) 273–276.
[41] P.D. Cary, D.S. King, C. Crane-Robinson, E.M. Bradbury, A. Rabbani, G.H. Goodwin, E.W. Johns, Structural studies on two high-mobility-group proteins from calf thymus, HMG-14 and HMG-20 (ubiquitin), and their interaction with DNA, Eur. J. Biochem. 112 (1980) 577–580.
[42] G. Gemmecker, W. Jahnke, H. Kessler, Measurement of fast proton exchange rates in isotopically labeled compounds, J. Am. Chem. Soc. 115 (1993) 11620–11621.
[43] M.H. Abraham, R.J. Abraham, J. Byrne, L. Griffiths, NMR method for the determination of solute hydrogen bond acidity, J. Org. Chem. 71 (2006) 3389–3394.
[44] J. Kärger, H. Pfeifer, W. Heink, Principles and application of self-diffusion measurements by NMR, in: W.S. Warren (Ed.), Advances in Magnetic Resonance, 12, Academic Press, New York, 1988, p. 1.
[45] J. Yan, A.D. Kline, H. Mo, E.R. Zartler, M.J. Shapiro, Epitope mapping of ligand–receptor interactions by diffusion NMR, J. Am. Chem. Soc. 124 (2002) 9984–9985.
[46] H. Koskela, O. Heikkinen, I. Kilpeläinen, S. Heikkinen, Rapid and accurate processing method for amide proton exchange rate measurement in proteins, J. Biomol. NMR 37 (2007) 313–320.